Hybrid Collagenase Nanocapsules for Enhanced Nanocarrier Penetration in Tumoral Tissues.

María Rocío Villegas[a,b], *Alejandro Baeza*[b,a]* *and María Vallet-Regí*[a,b]*

[a] Dpto. Química Inorgánica y Bioinorgánica. UCM. Instituto de Investigación Sanitaria Hospital 12 de Octubre i+12. Plaza Ramón y Cajal s/n, Madrid (28040), Spain.

[b] Centro de Investigación Biomédica en Red de Bioingeniería, Biomateriales y Nanomedicina (CIBER-BBN). Av Monforte de Lemos, 3-5, Madrid, Spain.

*Corresponding autor e-mail: abaezaga@ucm.es, vallet@ucm.es

ABSTRACT

Poor penetration of drug delivery nanocarriers within dense extracellular matrices constitutes one of the main liabilities of current nanomedicines. The conjugation of proteolytic enzymes on the nanoparticle surface constitutes an attractive alternative. However, the scarce resistance of these enzymes against the action of proteases or other aggressive agents present in the blood stream strongly limits their application. Herein, a novel nanodevice able to transport proteolytic enzymes coated with an engineered pH-responsive polymeric is presented. This degradable coat protects the housed enzymes against proteolytic attack at the same time that it triggers their release under mild acidic conditions, usually present in many tumoral tissues. These enzyme

nanocapsules have been attached on the surface of mesoporous silica nanoparticles, as nanocarrier model, showing a significatively higher penetration of the nanoparticles within 3D collagen matrices which housed Human Osteosarcoma cells (HOS). This strategy can improve the therapeutic efficacy of the current nanomedicines allowing a more homogeneous and deeper distribution of the therapeutic nanosystems in cancerous tissues.

Keywords: Tumoral tissue penetration, collagenase nanocapsules, nanomedicine, mesoporous silica nanodevices and hybrid nanocarriers.

INTRODUCTION

Nanoparticles have become a powerful weapon in the fight against cancer due to their passive accumulation within solid tumors (EPR effect).[1] This effect is caused by the distinctive tumoral blood vessels which present large pores and fenestrations of few hundred nanometers.[2] Thus, when the nanoparticles reach the tumoral zone, they are able to escape from these highly permeable blood vessels producing the accumulation in the diseased tissue.[3] Despite the huge importance of reaching the tumoral area, this is only the first step. The extravasated nanocarrier should be able to penetrate deeper into the solid tumor if a high therapeutic efficacy is pretended. Unfortunately, there are several physiological and physical barriers that should be overcome in order to achieve a homogeneous nanocarrier distribution in the entire malignant tissue.[4] Tumoral tissues exhibit elevated interstitial fluid pressure (IFP) which hampers the convective transport making diffusion the *de facto* sole transport mechanism for nanocarriers. Moreover, solid tumors usually present extracellular matrices (ECM) denser than healthy tissues, with higher collagen

content which hinders even more the nanocarrier diffusion.[5] The lack of an efficient nanoparticle distribution throughout all the diseased tissue reduces considerably the therapeutic efficiency of the nanomedicines and is one of their main liabilities.[6] Different strategies have been postulated in order to overcome this limitation. Thus, the nanocarrier surface decoration with cell penetrating peptides (CPP) in combination with magnetic field guidance[7] and even the use of self-propelled devices have been described to achieve a higher penetration in 3D tissues.[8] A simpler approach consists in the local administration of proteolytic enzymes prior to the nanocarrier treatment, which has demonstrated a significant nanoparticle penetration enhancement within the tumoral tissue.[9] Different proteolytic enzymes such as collagenase or bromelain have been directly anchored on the nanoparticle surface improving their diffusion in comparison with non-functionalized particles.[10,11] However, enzymes are labile entities which can suffer a rapid degradation in living tissues by the action of proteases or other aggressive agents present in the blood stream. Even the attachment method can compromise the enzymatic activity as a consequence of conformational changes or active site blockage.[12] Lu *et al.*[13,14] have reported an interesting strategy which consists in the enzyme encapsulation into polymeric nanocapsules in order to improve their resistance and to preserve their activity during longer times. Our research group has described the attachment of enzyme nanocapsules onto the nanoparticle surface for the development of devices able to generate *in situ* cytotoxic compounds[15] and also for the propulsion of nano- and micromotors.[16] Herein, we describe the design and attachment of hybrid collagenase-polymeric nanocapsules on the surface of mesoporous silica nanoparticles in order to improve their penetration within 3D collagen matrices with tumoral cells embedded within the network, which mimic tumoral tissues. These polymeric nanocapsules protect the enzyme against proteolytic degradation and hydrolysis

during longer times improving enzyme performance while allowing higher matrix degradation and therefore, deeper penetration within the tissue (**Scheme 1**).

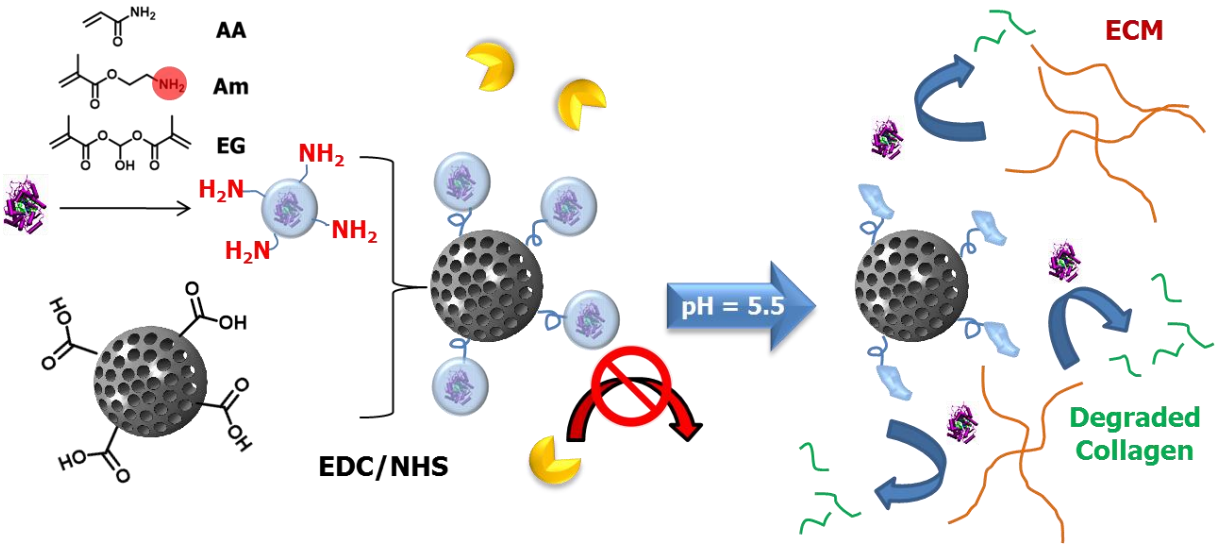

Scheme 1. Synthesis and mechanism of pH-responsive polymeric nanocapsules for enhanced extracellular matrix degradation and tumoral tissue penetration.

RESULTS AND DISCUSSION

Synthesis and performance evaluation of the collagenase nanocapsules.

Collagen is the most abundant component of the extracellular matrix. Thus, collagenase is one of the most suitable enzymes for ECM degradation. As mentioned above, a polymeric coating was built around the enzyme in order to preserve the activity against aggressive agents. The enzyme substrate is a big molecule and therefore, the enzyme should be released from the capsule in order to be active for efficient collagen degradation. For this reason, a pH-responsive polymeric nanocapsule has been designed. This polymer coating undergoes slow degradation at physiological conditions (pH = 7) but exhibits a rapid hydrolysis at mild acidic conditions (pH =

5.5) which are naturally present in many tumoral tissues, as a consequence of their accelerated metabolism and the hypoxic environment.[17] Thus, the enzyme will stay in an inactive stage until the pH becomes acidic, which will trigger the enzyme release with the subsequent collagen matrix degradation.

Collagenase nanocapsules (Col-nc) were synthesized forming a polymeric coating around the native collagenase (Col) by radical polymerization employing a monomer mixture of acrylamide (AA) as structural monomer, hydrochloride salt of 2-aminoethylmethacrylate (Am) in order to provide amino groups on the capsule surface and ethylene glycol dimethacrylate (EG) as pH-cleavable cross-linker. Different conditions were tested until the following optimal capsule formation parameters were found: monomer/protein molar ratio of 1:2025 and AA:Am:EG ratio (7:6:2). Thus, homogeneous protein nanocapsules were obtained with a diameter size around 50 nm according to Dynamic Light Scattering (DLS) and Transmission Electron Microscopy (TEM). The spherical morphology and size of the capsules was confirmed by Atomic Force Microscopy (AFM) (**Figure 1**).

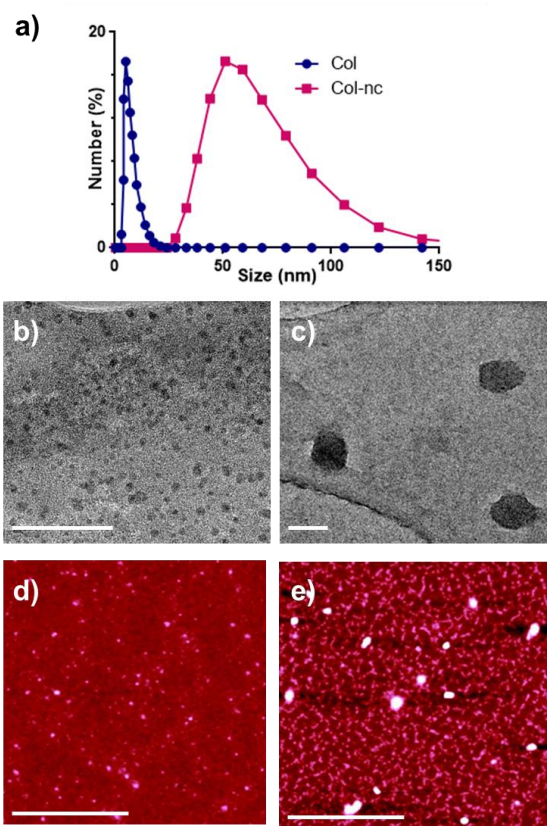

Figure 1. a) DLS of Col and Col-nc, b-c) TEM images of Col and Col-nc respectively, stained with phosphotungstic acid as contrast agent (scale bars correspond to 50 nm) and d-e) AFM of Col and Col-nc, respectively (scale bars correspond to 1 μm).

The presence of free amino groups on the capsule surface was confirmed by fluorescamine assay. The enzymatic activity of the capsules was determined using a commercial kit (EnzCheck Gellatinase/Collagenase, Molecular Probes®) which is based in the measurement of the fluorescein released when fluorescently labeled gelatin was exposed to enzyme degradation. After the encapsulation process, the enzymatic activity suffers a drastic reduction of around 50% which indicates that the polymeric coating significatively hampers the collagen degradation by the encapsulated enzyme (**Figure S1a**).

This fact confirms that the enzyme should be released in order to achieve an efficient degradation of the collagen matrix, as it was mentioned above. For this reason, EG was employed as pH-cleavable cross-linker. This molecule exhibits rapid hydrolysis under mildly acidic conditions, compromising the stability of the whole capsule and hence releasing the housed enzyme. The pH-responsive nature of the capsule was evaluated by DLS suspending the capsules at different pH values, 7.0 and 5.5 respectively, during 2 hours. After this time, the capsule exposed to acidic pH was completely broken showing the same hydrodynamic diameter by DLS as the native enzyme, whereas the capsule exposed to neutral pH did not suffer any size modification. Interestingly, the enzymatic activity was almost fully recovered after the acidic treatment but it was kept at 50% when the sample was maintained at pH = 7. These results are consistent with a complete release of the trapped enzyme (**Figure 2**).

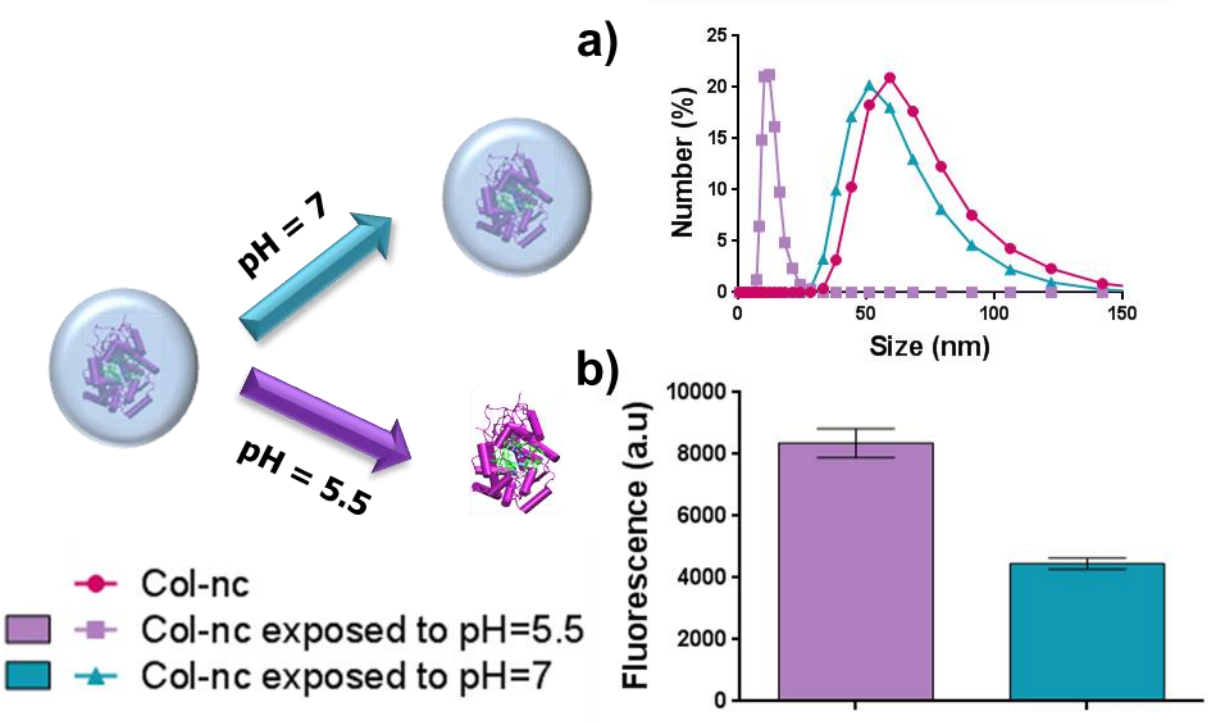

Figure 2. pH-responsive behavior of Col-nc, a) DLS measurements of Col-nc exposed to pH = 5.5 and 7, (purple and cyan lines, respectively) and b) Fluorescein released by a fluorescently

labeled collagen matrix treated with Col-nc previously exposed to pH = 5.5 and pH =7, (purple and cyan lines, respectively).

Attachment of collagenase nanocapsules on the nanocarrier surface.

Mesoporous silica nanoparticles (MSNs) have been chosen as nanomedicine model due to the excellent properties of this material such as high loading capacity and excellent biocompatibility, among others.[18,19] Thus, MSNs were synthesized following the modified Stöber method reported elsewhere.[20] According to DLS and TEM, the particles show a homogeneous size distribution centered around 140 nm which is convenient for their application as drug nanocarriers.[21] In order to provide anchoring points for the protein nanocapsules, the surface of the particles was decorated with carboxylic groups by condensation of 4-(trietoxisililetilene)succidimide with the silanol groups on the surface, followed by hydrolysis in acidic medium. The presence of carboxylic groups was confirmed by the apparition of the characteristic C=O band at 1710 cm^{-1} in the Fourier-Transform Infrared (FT-IR) spectrum and by Thermogravimetric Analysis (TGA). According with the DLS measurements, the particle size was maintained during this functionalization process (**Figure S2**).

Enzyme nanocapsules were covalently grafted on the MSNs surface through the well-known carbodiimide chemistry. Thus, the carboxylic groups present on the MSN were transformed into activated esters through the reaction with *N*-(3-Dimethylaminopropyl)-*N′*-ethylcarbodiimide hydrochloride (EDC) and *N*-Hydroxysuccidimide (NHS). Then, the presence of free amino groups on the capsule surface produces their attachment on the particle surface by the formation of highly stable amide bonds producing the complete material (MSN-Col-nc). The same reaction

was carried out using native collagenase (MSN-Col) as control in order to compare the performance and stability of both systems. In both cases, FTIR spectra show a slight decrease in the carboxylic acid band at 1710 cm^{-1} and the appearance of two bands at 1650 and 1568 cm^{-1} which correspond to amide bond formation and the protein. DLS measurements showed a size increase of around 50 nm, which corresponds to a discrete attachment of enzyme nanocapsules instead of to a complete covering of the entire surface (**Figure S2**). The conjugation of Col and Col-nc on the surface was confirmed by TEM using phosphotungstic acid as staining agent in order to increase the electron opacity of the organic material. In these images, the presence of the native enzymes attached on the silica surface is clearly visible as dark spots (**Figure 3b**) which are not present in naked MSN (**Figure 3a**). In the case of mesoporous silica particles decorated with collagen nanocapsules (MSN-Col-nc) these enzyme capsules are clearly visible attached on the particle surface, even keeping their round shape morphology (**Figure 3c-d**). TGA measurements and Sulfur analysis of the MSN-Col and MSN-Col-nc did not exhibit significative differences between them, showing in both cases around 6-8 % of grafted organic material. It is worth to note that MSN-Col-nc present high colloidal stability in aqueous media, being stable over time (**Figure S3**).

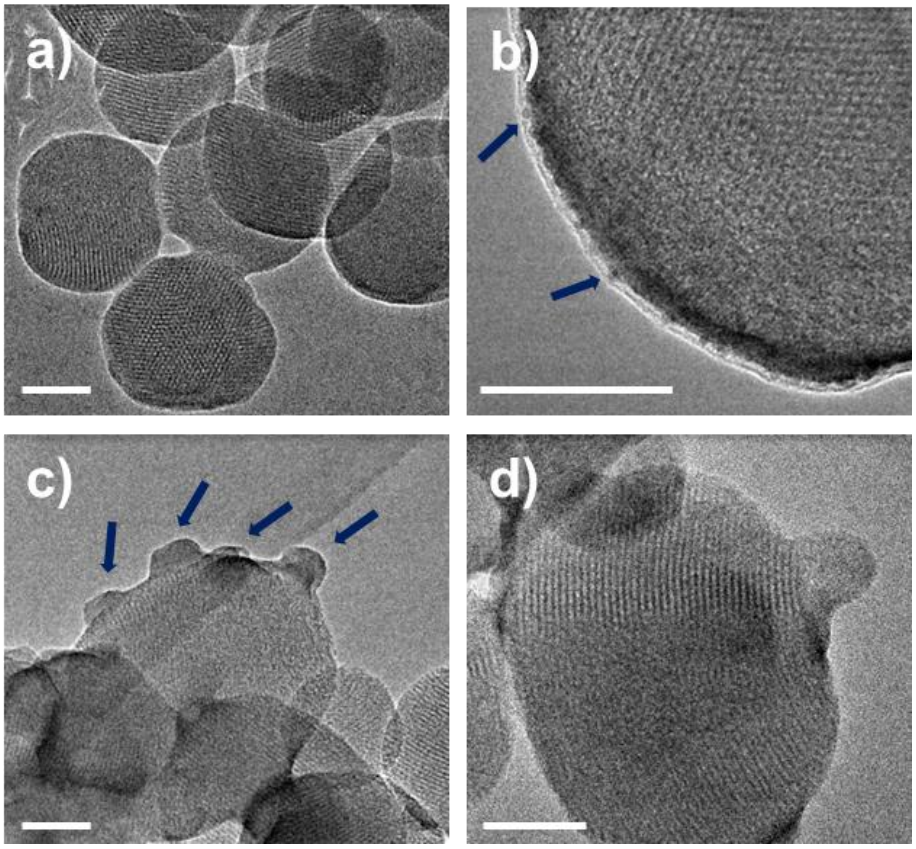

Figure 3. TEM images of a) MSN b) MSN-Col and c-d) MSN-Col-nc. Scale bars correspond to 50 nm. Blue arrows point out the presence of Col and Col-nc. Due to the stochastic nature of the grafting procedure, the collagen nanocapsules are randomly distributed on MSN surface.

Stability of MSN-Col-nc

Obviously, MSN-Col initially presents higher enzymatic activity than MSN-Col-nc (**Figure S1b**) mainly by two reasons, first the absence of a polymeric coat as it has been mentioned above and secondly, the higher steric hindrance of the capsules which causes a lower enzyme nanocapsules grafting in comparison with the native protein attachment. However, despite this initial advantage, the enzymatic activity of MSN-Col decreases in a short period of time when

the samples are suspended in a PBS buffer solution at pH = 7 and 37 ºC whereas the activity increases to double its initial value in the case of MSN-Col-nc. This behavior proves that the polymeric coat which wraps the enzyme suffers hydrolysis and the housed enzymes are slowly released or exposed fully recovering their capacity to digest collagen after longer periods of time (**Figure 4a**). It is important to remark that a similar amount of free enzyme almost completely loses its activity after a short incubation time of two hours in these conditions. One important role which should be played by the polymeric coat consists in the protection of the encapsulated enzyme against proteolytic attack, because the lack of stability against proteases is the main limitation on the use of proteins in clinical applications.[22] In order to compare the stability against proteases, samples MSN-Col and MSN-Col-nc were suspended at 37 ºC in a solution of PBS (pH = 7) which contains 1 $mg \cdot mL^{-1}$ of Protease from *Streptomyces griseus*. The results indicate that material with the uncoated enzyme lost more than 60% of its enzymatic activity after 3 hours while the sample with enzyme nanocapsules kept intact their activity (**Figure 4b**). All these experiments evidence the protective role of the polymeric nanocapsules.

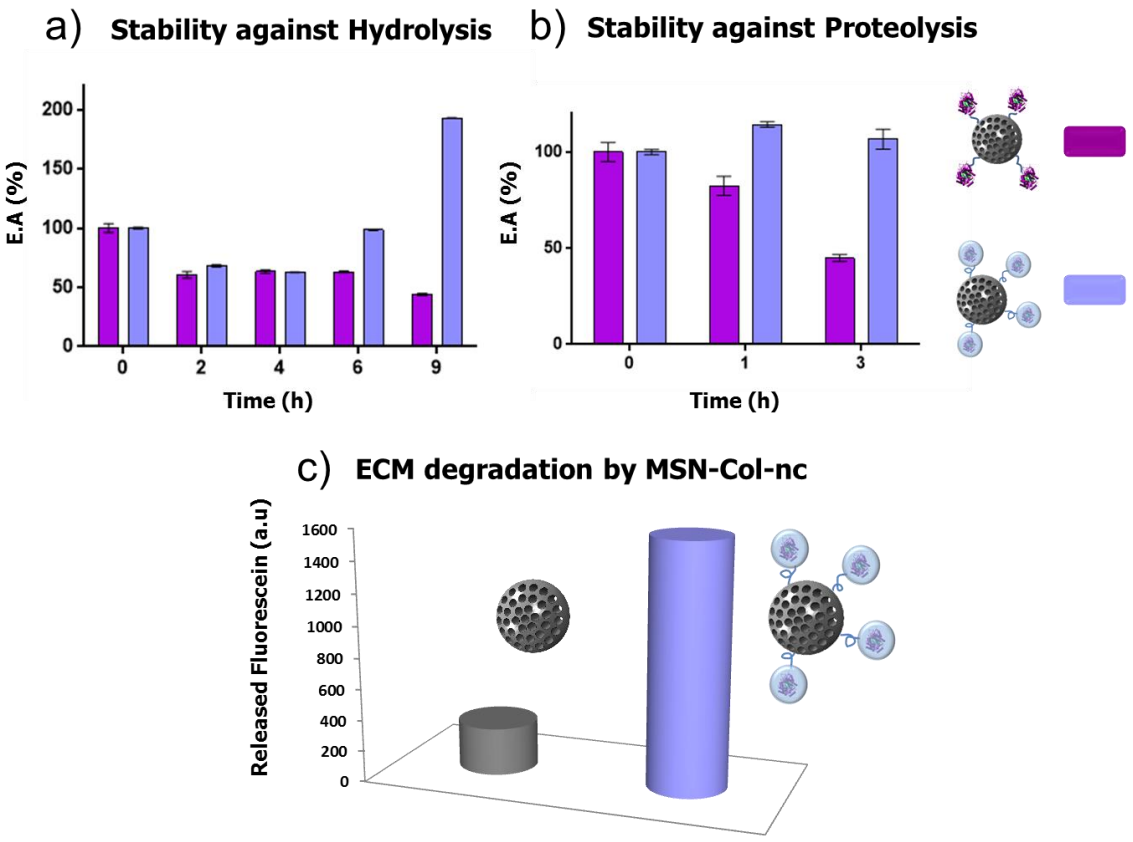

Figure 4. Stability test of MSN-Col and MSN-Col-nc against a) hydrolysis and b) Proteolytic attack c) ECM degradation by MSN-Col-nc.

EMC degradation capacity of MSN-Col-nc

The capacity of the protein capsules attached on the particle surface to degrade the extracellular matrix was initially tested using a 3D collagen matrix formed by MaxGel^{TM}ECM. This 3D matrix is composed by several human extracellular matrix components such as collagen, laminin, fibronectin, tenascin, elastin, and a number of proteoglycans and glycosaminoglycans which mimic the matrices present in human living tissues.[11] The proteins which form the 3D matrix were previously stained with fluorescein isothiocyanate (FITC) in order to monitorize the

matrix degradation through the measurement of the fluorescein released after addition of the nanoparticles. Naked MSN, which shows negligible enzymatic activity (**Figure S4**) was used as control. A suspension of 1 $mg \cdot mL^{-1}$ of MSN-Col-nc and MSN respectively, was carefully added on top of the fluorescent 3D gels and both samples were incubated at 37 ºC during 24 hours. After this time, a strong fluorescence was observed in the case of MSN-Col-nc whereas a scarce fluorescence was observed in the case of naked MSN (**Figure 4c**). The particles decorated with collagenase nanocapsules present a five-fold increase in the ECM degradation in comparison with the non-functionalized ones.

Penetration capacity of MSN-Col-nc in 3D-Human Osteaosarcoma-seeded collagen gels.

A 3D-tumoral tissue model was prepared in order to study the MSN-Col-nc performance in a more realistic model which takes into account the influence that could exert the presence of tumoral cells embedded within the matrix. To this end, a 3D-collagen gel which contains Human Osteosarcoma cells (HOS) was synthesized following a slightly modified procedure reported elsewhere (**Figure S5**).[7] This matrix shows similar consistency to real human tissue and the presence of embedded tumoral cells provides a realistic environment for testing the penetration capacity of nanocarriers clothed with these enzyme capsules. In order to visualize the penetration of the nanoparticles within the collagen gel, MSNs were synthesized carrying fluorescein molecules covalently grafted within their structure following a procedure reported elsewhere.[27] The stability of the fluorescein molecules covalently grafted within the silica matrix was evaluated suspending a certain solution of fluorescent MSN in PBS buffer at pH =7 and 37 ºC and measuring by fluorescence spectroscopy the fluorescein lixiviated in the supernatant and

the fluorescence remained in the particles over time (**Figure S6**). The absence of lixiviated fluorescein confirms the stability of the FITC covalent grafting protocol. After this, collagenase and collagenase nanocapsules were grafted on the fluorescent MSN surface through the same conjugation method employed for non-fluorescent MSN. A suspension of fluorescent MSN and MSN-Col-nc, respectively (25 $\mu g \cdot mL^{-1}$) was carefully placed on top of the 3D-gels; the penetration capacity of each carrier was evaluated by confocal fluorescence microscopy after 24 hours of incubation. The results indicated that the naked particles were not able to penetrate within the gel and remained fixed on the top layer, whereas MSN-Col-nc exhibited an improved penetration within the 3D-matrix (**Figure 5a-b**). It is worthy to point out that if the concentration of MSN-Col-nc was doubled, a drastic decrease of the matrix thickness was observed up to reach only one third of the original size (**Figure 5c**). This fact indicates that the released collagenase diffuses throughout the matrix causing a higher collagen digestion as a consequence of their higher concentration in this case.

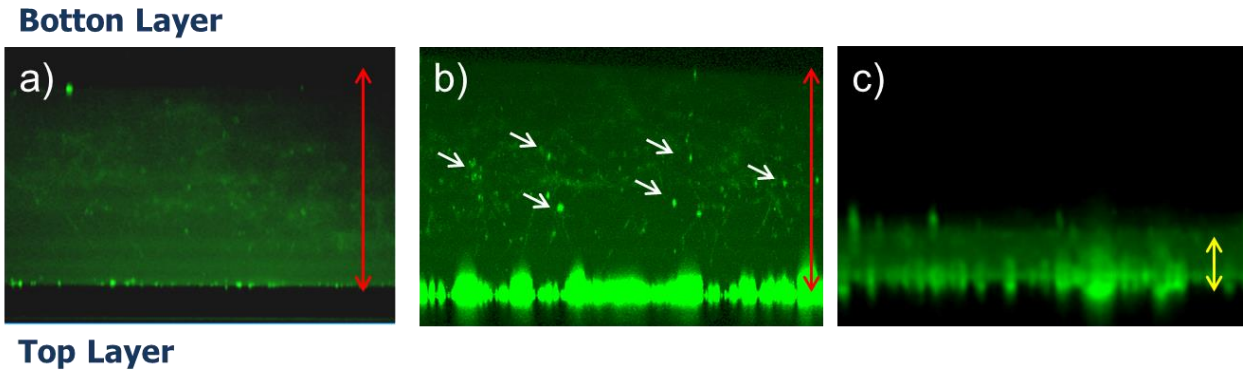

Figure 5. Penetration in 3D-HOS-seeded collagen gels of a) MSN and b) MSN-Col-nc using a particle concentration of 25 $\mu g \cdot mL^{-1}$, respectively (White arrows indicate the presence of clusters of MSN-Col-nc). c) Penetration of MSN-Col-nc using a concentration of 50 $\mu g \cdot mL^{-1}$. Red

arrows correspond to a gel thickness of 740 μm. Yellow arrow corresponds to a gel thickness of 280 μm.

Cytotoxicity studies of MSN-Col-nc.

It has been reported that collagenase, both alone[23] or conjugated on the surface of different nanoparticles[24,25] causes very low toxicity in human cells. Additionally, MSN is also a biocompatible material.[26] However, our system is composed by a novel type of collagenase nanocapsules grafted on the MSN surface and its cytotoxicity should be evaluated. Thus, HOS cells were incubated in the presence of a fixed concentration of naked MSN and MSN-Col-nc (25 $\mu g \cdot mL^{-1}$, which is the optimal concentration for tissue penetration) during 24 hours and their cell viability was evaluated measuring the Lactate deshydrogenase (LDH) released in the media. As shown in **Figure 6a**, the exposition to naked particles and particles decorated with the enzyme nanocapsules did not cause higher LDH release in comparison with the negative control which corresponds to untreated cells. In order to simulate a highly cytotoxic material, as positive control, the cells were exposed to a solution of Triton X (2%) which caused their complete destruction and a subsequent LDH increment of more than four times. The absence of cytotoxicity caused by the exposition to these materials was confirmed using the standardized cell viability test by MTS reduction that exhibit similar values in all systems (**Figure 6b**). These results indicate that neither of the materials provokes a substantial cell death.

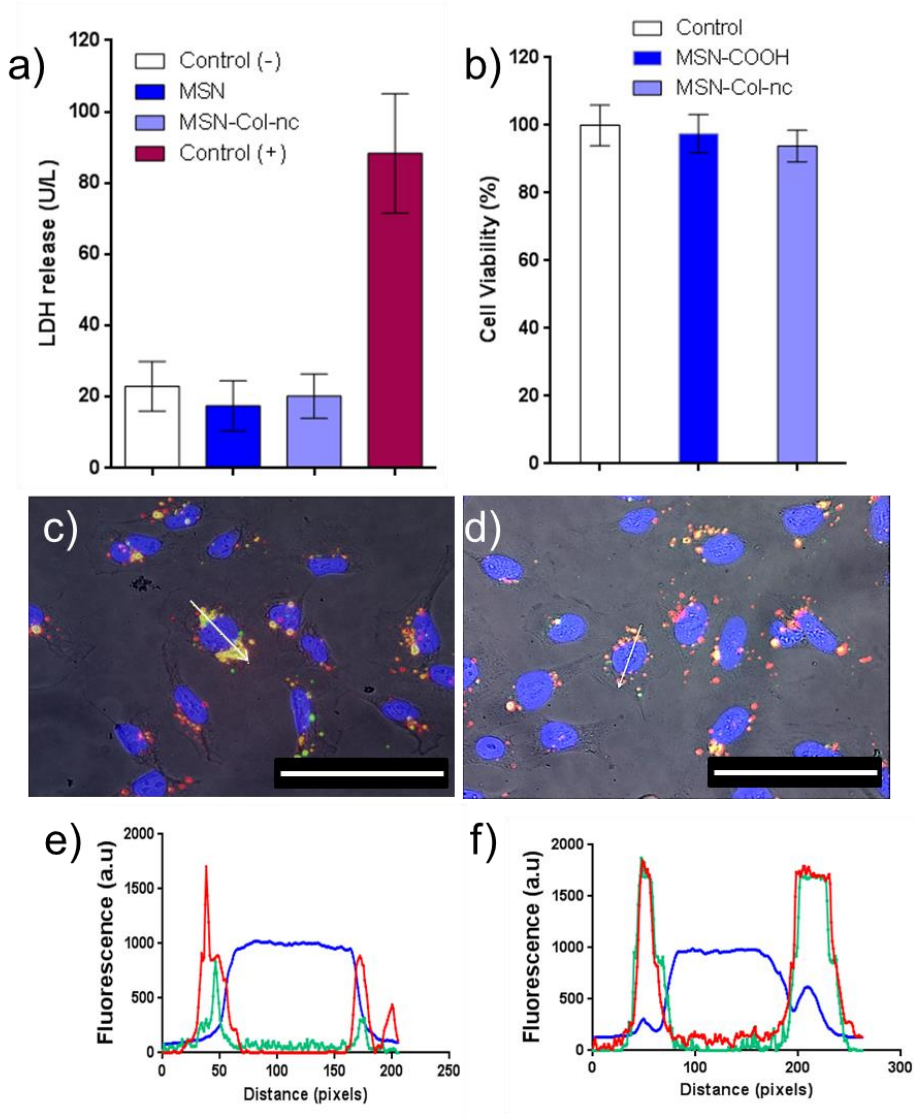

Figure 6. a) LDH assay of MSN and MSN-Col-nc where Control (-) are cells without treated with particles and Control (+) are cells lysed with Triton X in order to simulate full cytotoxicity. b) Cell viability assay by MTS test of MSN and MSN-Col-nc c-d) Merged microscopy images of HOS cells incubated with MSN and MSN-Col-nc labeled with fluorescein. Blue stain corresponds to cell nucleus, green stain corresponds to nanoparticles and red stain corresponds to lysosomes (Scale bar correspond to 100 µm). Each channel can be separately observed in Figure S7. e-f) Fluorescence intensity of each fluorophore emission wavelength along the white arrow

in c-d images (red pattern correspond to lysosomes, green pattern correspond to MSN and MSN-Col-nc and blue pattern correspond to cell nuclei).

In order to visualize if the nanoparticles were internalized within the tumoral cells, the lysosomes were stained using Cell Navigator^{TM} Lysosome Staining Kit showing that the nanoparticles were mainly located within these cell organelles (**Figure 6c-d**). Additionally these results were confirmed measuring independently the fluorescence intensity of each fluorophore obtaining a clear pattern which shows that nanoparticles are mainly located in the same place than lysosomes and outside the cell nuclei (**Figure 6e-f**).

CONCLUSIONS

In conclusion, a novel strategy to transport collagenase attached on the surface of a nanocarrier and to release it in a controlled manner has been presented. This approach is based on the synthesis of hybrid enzyme-polymer nanocapsules which have been engineered to exhibit slow enzyme release at physiological conditions or faster if the pH drops to mild-acidic values, which is characteristic of many tumoral tissues. Moreover, these capsules protect the enzymes against proteolytic attack by proteases, which is one of the main limitations of employing enzymes in living tissues, maintaining their activity during long times. Finally, the attachment of these enzyme capsules on the surface of a model nanocarrier has afforded a significant improvement of their penetration within a tumoral tissue model as a consequence of the abundant extracellular matrix degradation caused by the *in situ* released collagenase. These properties would be of paramount importance for clinical applications paving the way for the development of more efficient nanomedicines able to achieve deeper penetration and more homogeneous distribution within the tumoral tissues.

EXPERIMENTAL SECTION

Synthesis of Collagenase Capsule (Col-nc): $3.1 \cdot 10^{-5}$ mmol of collagenase was dissolved in 1 mL of $NaHCO_3$ buffer (0.01M pH = 8.5), previously deoxygenated three times for freeze-vacum-N_2 cycles, at room temperature. 0.035 mmol of acrylamide (AA), 0.026 mmol of 2-Aminometacrylate hydrochloride (Am) and 0.01 mmol of Ethylene glicol dimetacrylate (EG) were dissolved in 1 mL of deoxygenated $NaHCO_3$ (0.01M pH = 8.5) buffer and were added to the solution of collagenase. This mixture was stirred at 300 rpm for 10 min under nitrogen atmosphere at room temperature. Then, 0.013 mmol of ammonium persulfate and 0.002 mmol of *N,N,N',N'*-Tetramethyl ethylenediamine (TMDA) dissolved in 1 mL of the deoxygenated $NaHCO_3$ buffer (0.01M pH = 8.5) were added. The solution was stirred at 300 rpm for 90 min at room temperature under inert atmosphere. After this time, the encapsulated enzyme was purified by centrifugal separation with 10 kDa cut-of filters (AMICON Ultra-2mL 10KDa) and washed three times with $NaHCO_3$ buffer (0.01M pH = 8.5). The capsules of collagenase were preserved at 4 °C.

Synthesis of Mesoporus Silica Nanoparticles: 2.74 mmol of Hexadecyltrimethylammonium bromide (CTAB), 480 mL of water and 7 mmol of NaOH were stirred at 600 rpm at 80 °C. Then, 22.4 mmol of tetraethylortosilicate (TEOS) was added slowly during 20 minutes and upon addition, the mixture was stirred during two hours at 80 ºC. Then, the particles were collected by centrifugation and washed three times with water and ethanol. The surfactant was removed placing the particles in 500 mL of a solution of 95% ethanol, 5% water and 10 g NH_4NO_3 mL^{-1} at 80 °C during two hours under intense stirring. The same cycle was repeated two times more

in order to remove all the surfactant. The nanoparticles were dried under vacuum and preserved at room temperature.

For penetration studies within 3D gels, fluorescent nanoparticles were synthesized following an analogous protocol described elsewhere.[27] Briefly, FITC (1mg) and APTES (2,2 μL) were dissolved in the minimum volume of EtOH and the mixture was stirred at room temperature for 2 hours under N_2 atmosphere. Then, this solution was mixed with 22. 4 mmol of TEOS and the particles were synthesized following the same method mentioned above.

Synthesis of acid-funcionalizated Silica Nanoparticles (MSN): 500 mg of the particles obtained above and 1.34 mmol of anhydrous 4-(trietoxisililetilene)succidimide were suspended in 50 mL of dry toluene under inert atmosphere at 110 °C under intense stirring overnight. Then, the nanoparticles were collected by centrifugation and washed with toluene, tetrahydrofuran and finally with water, in order to hydrolyze the succinic anhydride providing the carboxylic acid groups. The particles were dried under vacuum and preserved at room temperature.

Attachment of Native Collagenase on Silica Nanoparticles (MSN-Col): A suspension of 50 mg of MSN in 2 mL PBS (pH = 7) was treated with 0.03 mmol of *N*-(3-Dimethylaminopropyl)-*N*′-ethylcarbodiimide hydrochloride (EDC) and 0.04 mmol of *N*-Hydroxysuccidimide (NHS). The pH was fixed to pH = 8.5 adding 0.06 mmol of sodium carbonate. The sample was placed in an orbital stirrer at 400rpm during 10 min and after this time, $3.1 \cdot 10^{-4}$ mmol of collagenase were added and the mixture was stirred during 4h. The sample was collected by centrifugation and washed three times with PBS. The sample was preserved at 4 ºC.

Attachment of Collagenase nanocapsules on Silica Nanoparticles (MSN-Col-nc): A suspension of 50 mg of MSN in 2 mL PBS (pH = 7) was treated with 0.03 mmol of *N*-(3-Dimethylaminopropyl)-*N*′-ethylcarbodiimide hydrochloride (EDC) and 0.04 mmol of *N*-

Hydroxysuccidimide (NHS). The pH was fixed to pH = 8.5 adding 0.06 mmol of sodium carbonate. The sample was placed in an orbital stirrer at 400rpm during 10 min and after this time, 10 mg of collagenase nanocapsules were added and the mixture was stirred during 4 h. The sample was collected by centrifugation and washed three times with PBS. The sample was preserved at 4 ºC.

Enzymatic activity measurements: The enzymatic activity of all samples was evaluated using and following the protocol EnChek®Gelatinase/Collagenase Assay Kit. For this experiment, 80 µl of collagenase buffer 1x, 20 µL of Collagen-FITC and 100 µL of each sample were used.

Study pH Responsive of MSN-Col-nc:

Size measurements by DLS: 100 µL of the encapsulated collagenase (Col-nc) was dissolved in 2 mL of HPLC water. The initial hydrodynamic diameter of the capsules was characterized by DLS and it was compared with the size of the native collagenase (Col). 1 mL of this solution was placed into a pur-A-lyzer (6 kDa) which was submerged in a flask with 200 mL of PBS Buffer pH = 7.0 at 37 °C with magnetic stirring for 2 h. Another batch of 1 mL was similarly treated but in this case using a solution of 200 mL of PBS Buffer pH = 5.5. After this time, the changes in the hydrodynamic diameter of both batches were evaluated by DLS.

Enzymatic Activity: 150 µL of the encapsulated collagenase (Col-nc) was suspended in 1mL of PBS buffer 0.01 M pH = 7. One batch of 400 µL of this solution was placed into a pur-A-lyzer (6 kDa) submerged in 200 mL of the same buffer at 37 °C with magnetic stirring during 4h. Another batch was placed into a pur-A-lyzer (6 kDa) submerged in 200 mL of PBS Buffer pH = 5.5 at 37 °C for 3 h and 1 h more in PBS buffer 0.01 M pH = 7 at 37 ºC in order to equilibrate the

pH before performing the enzymatic activity measurements. Then, both batches were diluted 1:100 in PBS and then the enzymatic activity of the capsules solution was evaluated.

Study of the Enzymatic Activity of MSN-Col and MSN-Col-nc:

Stability during the time: 2 mg of silica nanoparticles functionalized with native and encapsulated collagenase (Col and Col-nc, respectively) were suspended in PBS 0.01M at pH = 7 at 37 ºC and their enzymatic activity was studied at different times.

Study Enzymatic activity against proteases: Two batches of 1 mg of the MSN-Col-nc and MSN-Col were suspended respectively in a solution of 1mg·mL^{-1} Protease from *Streptomyces griseus* in PBS Buffer 0.01 M (pH = 7). Both samples were incubated at 37 °C during the corresponding time and after this time, they were washed ten times with the same buffer in order to remove the proteases. Then, the enzymatic activity of the nanoparticles was measured using the protocol mentioned above.

ECM degradation by MSN-Col-nc: MaxGel^{TM}ECM was diluted 1:2 in a cold solution of 0.0026 mmol/mL of Fluorescein isomer I (FITC) in PBS 0.01 M pH = 7. Then the solution was pipetted into 96 well plates and incubated for 5h at 37°C in order to promote the gelation. Once the gel was formed, the supernatant was removed and the gel was gently washed until the observation of neglictable fluorescence in the supernatant. 200 µL of a suspension of 1 mg·mL^{-1} of MSN and MSN-Col-nc in PBS 0.01 M pH = 7 respectively, was pipetted on the ECM gel and incubated at 37 °C during 24 h. Then, the fluorescence of supernatant was analyzed.

Preparation of 3D-Human Osteaosarcoma-seeded collagen gels: 2 mL of rat tail CollagenType I and 0.6 mL of complete medium (Dulbecco's modified eagle's medium complemented with 10% of FBS) were mixed in cold and 100µL of sodium hydroxide were added to obtain a mixture of neutral pH. To this solution, 0.5 mL of FBS, 0.5mL of complete

medium and 0.5 mL of a solution of cells of concentration HOS $1:10^6$ cell/mL was added, keeping the temperature at 0 ºC. The mixture was pipetted into 12 well plates (0.5mL/well) and incubated at 37 °C at 5% CO_2 atmospheric concentration for 1 h to promote gel formation. Then 500 µL of complete medium was added in each well and the gel was incubated at 37 °C at 5% CO_2 atmospheric concentration overnight. After this time, a needle was run around the edge of each solid gel to detach it from the plastic and 0.5 mL of complete medium was added. Gels were used in experiments four days after detachment to allow full gel contraction.

Study of penetration of MSN-Col-nc in HOS-collagen gels: To study the penetration of nanocarriers in 3D gels with cells HOS embedded, the medium which cover the gels was removed and the corresponding amount of suspended MSN and MSN-Col-nc (1 mg $\cdot mL^{-1}$) was added on top of each gel. These samples were incubated at 37 °C at 5% CO_2 atmospheric concentration during 24h. Then, the supernatant was removed and the gel was fixed at 4 ºC during 1 h with 0.5 ml of a solution of glutaraldehyde at 2.5 % of concentration. Then, confocal fluorescence microscope (using 10x magnifications) was used to determine the penetration by z-stack images of each gel, composed of sequential images taken 2 µm apart. Each compressed z-stack was analyzed and used for statistical analysis and graphical representation.

Cell viability studies:

The cytotoxicity of nanocarriers was evaluated using the standard LDH activity test and the MTS reduction assay protocol. For this study 20000 cells HOS$\cdot cm^{-2}$ were seeded into each well of a 24 well plate, 0.5mL of complete media was added to each well and the cells were cultured at 37 °C at 5% CO_2 atmospheric concentration for 24h. Then, the cells were incubated with the corresponding sample MSN and MSN-Col-nc, at 25 µg$\cdot mL^{-1}$ or without particles in the case of controls (+) and (-), during 24 h at 37 °C at 5% CO_2 atmospheric concentration. In the case of

control (+) a suspension of Triton X (2%) was added and the cells were incubated during 2h. After this time, the supernatant was collected for measuring the extracellular LDH activity. The cells were washed with 0.5 mL of PBS twice and 0.3 mL of a solution of 2 mL of MTS in 10 mL of complete medium was added. The cell culture was incubated at 37 °C at 5% CO_2 atmospheric concentration for 4h and then the supernatant was collected for the MTS assay.

Lactate dehydrogenase (LDH) assay: Extracellular LDH activity was measured using 33 µL of supernatant and 1000 µL of the kit for Quantitative determination of LDH (Spinreact®). The LDH activity was measured by spectrophotometer at 340 nm in the culture medium following the manufacturer protocol.

MTS assay: The MTS (3-(4,5-dimethylthiazol-2-yl)-5-(3-carboxymethoxyphenyl)-2-(4-sulfophenyl)-2H-tetrazolium) reduction assay was performed using a commercial assay and following the manufacturer protocol (CellTiter® Aqueous One Solution Cell Proliferation Assay). The absorption of supernatant was measured at 490 nm using a microplate reader.

Fluorescence microscopy images of HOS exposed to MSN and MSN-Col-nc.

For this study, HOS cells were exposed during 24 h to the same nanoparticle concentration (25 $\mu g \cdot mL^{-1}$) of MSN and MSN-Col-nc covalently labeled with fluorescein as in the previously mentioned assays.

In order to visualize lysosomes, a staining kit (Cell Navigator™ Lysosome Staining Kit) was employed. Briefly, 20 µl of LisoBrite™ Red, 4.98 ml of Live Cell Staining Buffer and 5 ml of complete media were mixed. 600 µl of these dilutions were added into each well of a 24 well plate which contains the cells and they were incubated for 30 min at 37 ºC. Then, the supernatant was removed and the cells were washed with 0.5 mL of PBS twice. To visualize the cells nuclei, 600 µl of 1 µg/ml DAPI in methanol was added into each well and the cells were incubated for

1min at 37 ºC. Finally, the supernatant was removed and the cells were washed with 0.5 mL of PBS twice.

ASSOCIATED CONTENT

Supporting Information. Materials and Instruments descriptions, Enzymatic activity of Col and Col-nc, FTIR spectra, DLS, Z potential, TGA values, 3D-Human Osteaosarcoma-seeded collagen gel characterization, stability test of FITC on MSN and fluorescence microscopy images of the cells.

"This material is available free of charge via the Internet at http://pubs.acs.org."

AUTHOR INFORMATION

Corresponding Authors

* Dr Alejandro Baeza, abaezaga@ucm.es and *Prof. María Vallet-Regí, vallet@ucm.es

Dpto. Química Inorgánica y Bioinorgánica. Facultad de Farmacia. UCM. Plaza Ramón y Cajal s/n. Madrid, Spain.

Author Contributions

The manuscript was written through contributions of all authors. All authors have given approval to the final version of the manuscript.

ACKNOWLEDGMENTS

This work was supported by the Ministerio de Economía y Competitividad, through project MAT2012-35556, CSO2010-11384-E (Agening Network of Excellence). We also thank the X-ray Diffraction C.A.I. and the National Electron Microscopy Center, UCM.

REFERENCES

(1) Ediriwickrema, A.; Saltzman, W. M. Nanotherapy for Cancer: Targeting and Multifunctionality in the Future of Cancer Therapies. *ACS Biomater. Sci. Eng.* **2015**, *1*, 64–78.

(2) Maeda, H.; Nakamura, H.; Fang, J. The EPR Effect for Macromolecular Drug Delivery to Solid Tumors: Improvement of Tumor Uptake, Lowering of Systemic Toxicity, and Distinct Tumor Imaging in Vivo. *Adv. Drug Deliv. Rev.* **2013**, *65*, 71–79.

(3) Jain, R. K.; Stylianopoulos, T. Delivering Nanomedicine to Solid Tumors. *Nat. Rev. Clin. Oncol.* **2010**, *7*, 653–664.

(4) Florence, A. T. "Targeting" Nanoparticles: The Constraints of Physical Laws and Physical Barriers. *J. Control. Release* **2012**, *164*, 115–124.

(5) Netti, P. a; Berk, D. a; Swartz, M. a; Grodzinsky, a J.; Jain, R. K. Role of Extracellular Matrix Assembly in Interstitial Transport in Solid Tumors. *Cancer Res.* **2000**, *60*, 2497–2503.

(6) Lammers, T.; Kiessling, F.; Hennink, W. E.; Storm, G. Drug Targeting to Tumors: Principles, Pitfalls and (pre-) Clinical Progress. *J. Control. Release* **2012**, *161*, 175–187.

(7) Child, H. W.; Del Pino, P. a.; De La Fuente, J. M.; Hursthouse, A. S.; Stirling, D.; Mullen, M.; McPhee, G. M.; Nixon, C.; Jayawarna, V.; Berry, C. C. Working Together: The Combined Application of a Magnetic Field and Penetratin for the Delivery of Magnetic Nanoparticles to Cells in 3D. *ACS Nano* **2011**, *5*, 7910–7919.

(8) Kagan, D.; Benchimol, M. J.; Claussen, J. C.; Chuluun-Erdene, E.; Esener, S.; Wang, J. Acoustic Droplet Vaporization and Propulsion of Perfluorocarbon-Loaded Microbullets for Targeted Tissue Penetration and Deformation. *Angew. Chem. Int. Ed.* **2012**, *51*, 7519–7522.

(9) McKee, T. D.; Grandi, P.; Mok, W.; Alexandrakis, G.; Insin, N.; Zimmer, J. P.; Bawendi, M. G.; Boucher, Y.; Breakefield, X. O.; Jain, R. K. Degradation of Fibrillar Collagen in a Human Melanoma Xenograft Improves the Efficacy of an Oncolytic Herpes Simplex Virus Vector. *Cancer Res.* **2006**, *66*, 2509–2513.

(10) Kuhn, S. J.; Finch, S. K.; Hallahan, D. E.; Giorgio, T. D. Proteolytic Surface Functionalization Enhances in Vitro Magnetic Nanoparticle Mobility through Extracellular Matrix. *Nano Lett.* **2006**, *6*, 306–312.

(11) Parodi, A.; Haddix, X. S. G.; Taghipour, X. N.; Scaria, S.; Taraballi, F.; Cevenini, A.; Yazdi, I. K.; Corbo, C.; Palomba, R.; Khaled, S. Z.; Martinez, J. O.; Brown, B. S.; Isenhart, L.; Tasciotti, E. Bromelain Surface Modification Increases the Diffusion of Silica Nanoparticles in the Tumor Extracellular Matrix. *ACS Nano*, **2014**, *8*, 9874–9883.

(12) Mateo, C.; Palomo, J. M.; Fernandez-Lorente, G.; Guisan, J. M.; Fernandez-Lafuente, R. Improvement of Enzyme Activity, Stability and Selectivity via Immobilization Techniques. *Enzyme Microb. Technol.* **2007**, *40*, 1451–1463.

(13) Yan, M.; Du, J.; Gu, Z.; Liang, M.; Hu, Y.; Zhang, W.; Priceman, S.; Wu, L.; Zhou, Z. H.; Liu, Z.; Segura, T.; Tang, Y.; Lu, Y. A Novel Intracellular Protein Delivery Platform Based on Single-Protein Nanocapsules. *Nat. Nanotechnol.* **2010**, *5*, 48–53.

(14) Yan, L.; Du, J.; Yan, M.; Lau, M. Y.; Hu, J.; Han, H.; Yang, O. O.; Liang, S.; Wei, W.; Wang, H.; Li, J.; Zhu, X.; Shi, L.; Chen, W.; Ji, C.; Lu, Y. Biomimetic Enzyme Nanocomplexes: Use as Antidotes and Preventive Measures for Alcohol Intoxication. *Nat. Nanotechnol.* **2013**, *8*, 187-192.

(15) Baeza, A.; Guisasola, E.; Torres-Pardo, A.; González-Calbet, J. M.; Melen, G. J.; Ramirez, M.; Vallet-Regí, M. Hybrid Enzyme-Polymeric Capsules/Mesoporous Silica Nanodevice for In Situ Cytotoxic Agent Generation. *Adv. Funct. Mater.* **2014**, *24*, 4625–4633.

(16) Simmchen, J.; Baeza, A.; Ruiz-Molina, D.; Vallet-Regí, M. Improving Catalase-Based Propelled Motor Endurance by Enzyme Encapsulation. *Nanoscale* **2014**, *6*, 8907–8913.

(17) Danhier, F.; Feron, O.; Preat, V. To Exploit the Tumor Microenvironment: Passive and Active Tumor Targeting of Nanocarriers for Anti-Cancer Drug Delivery. *J. Control. Release* **2010**, *148*, 135–146.

(18) Baeza, A.; Colilla, M.; Vallet-Regí, M. Advances in Mesoporous Silica Nanoparticles for Targeted Stimuli-Responsive Drug Delivery. *Expert Opin. Drug Deliv.* **2015**, *12*, 319–337.

(19) Vallet-Regi, M.; Rámila, A.; del Real, R. P.; Pérez-Pariente, J. A New Property of MCM-41: Drug Delivery System. *Chem. Mater.* **2001**, *13*, 308–311.

(20) Hoffmann, F.; Cornelius, M.; Morell, J.; Froeba, M. Silica-Based Mesoporous Organic-Inorganic Hybrid Materials. *Angew. Chem. Int. Ed.* **2006**, *45*, 3216–3251.

(21) Mamaeva, V.; Sahlgren, C.; Linden, M. Mesoporous Silica Nanoparticles in Medicine-Recent Advances. *Adv. Drug Deliv. Rev.* **2013**, *65*, 689–702.

(22) Fágáin, C. Ó. Understanding and Increasing Protein Stability. *Biochim. Biophys. Acta - Protein Struct. Mol. Enzymol.* **1995**, *1252*, 1–14.

(24) Khawar, I. A.; Kim, J. H.; Kuh, H.-J. Improving Drug Delivery to Solid Tumors: Priming the Tumor Microenvironment. *J. Control. Release* **2015**, *201*, 78–89.

(25) Goodman, T. T.; Olive, P. L.; Pun, S. H. Increased Nanoparticle Penetration in Collagenase-Treated Multicellular Spheroids. *Int. J. Nanomedicine* **2007**, *2*, 265–274.

(26) Tang, F.; Li, L.; Chen, D. Mesoporous Silica Nanoparticles: Synthesis, Biocompatibility and Drug Delivery. *Adv. Mater.* **2012**, *24*, 1504–1534.

(27) Liong, M.; Lu, J.; Kovochich, M.; Xia, T.; Ruehm, S. G.; Nel, A. E.; Tamanoi, F.; Zink, J. I. *ACS Nano*, **2008**, *2*, 889-896.

Insert Table of Contents Graphic and Synopsis Here

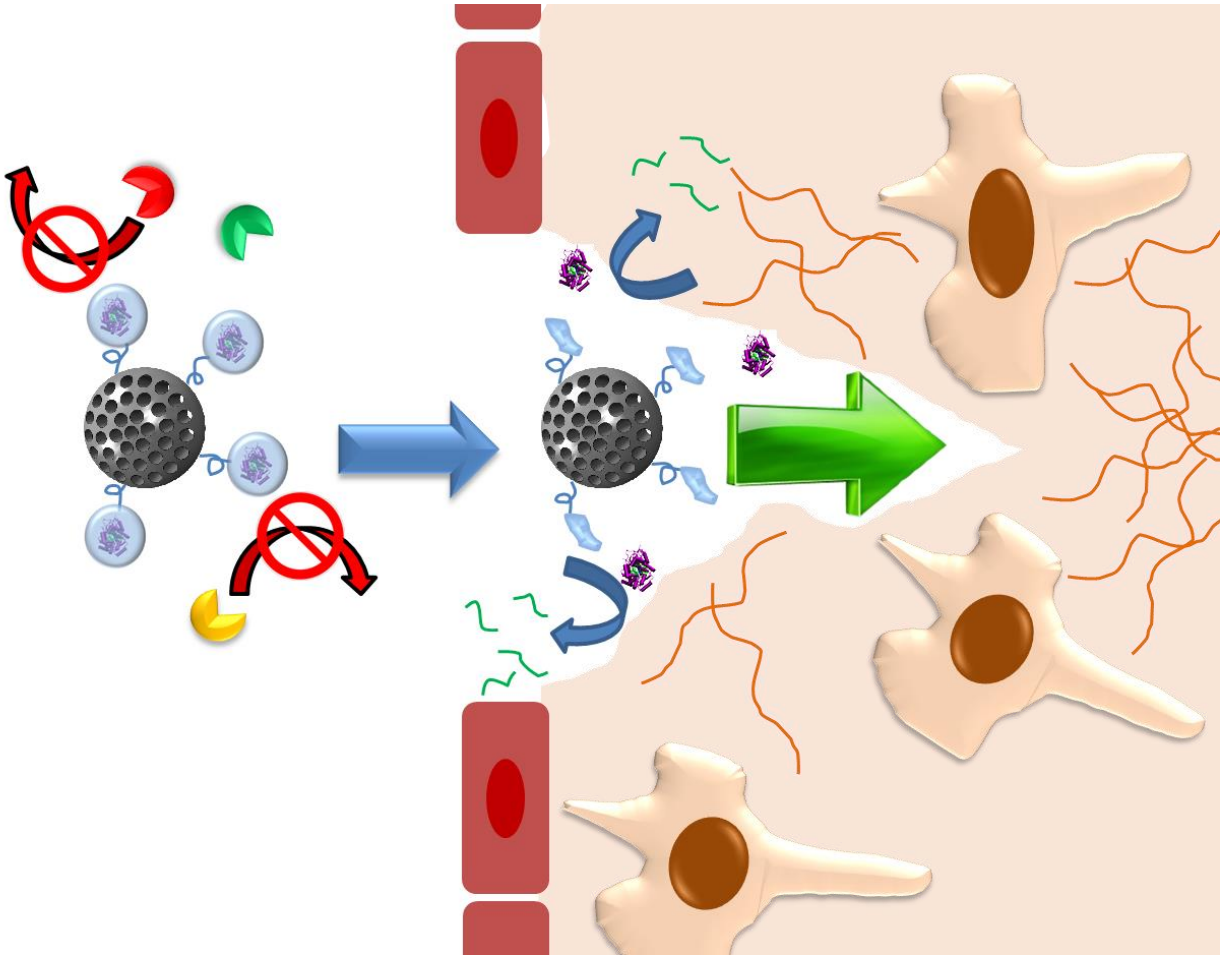

SYNOPSIS TOC. Enhanced 3D-tumoral tissue nanocarrier penetration by proteolytic enzymes housed within a degradable nanocapsules, which protect them against proteolytic attack at the same time that allows their release under mild acidic tumoral conditions.